TISSUE ENGINEERING: Part C
Volume 28, Number 4, 2022

DOI: 10.1089/ten.tec.2021.0191

termis
Tissue Engineering
& Regenerative Medicine
International Society

METHODS ARTICLE

Decellularization Detergents As Methodological Variables in Mass Spectrometry of Stromal Matrices

Giulia Remaggi,[1] Fulvio Barbaro,[2] Giusy Di Conza,[2] Giovanna Trevisi,[3] Carlo Bergonzi,[1] Roberto Toni,[2,4] and Lisa Elviri[1]

Collagens, elastin, fibrillin, decorin, and laminin are key constituents of the extracellular matrix and basement membrane of mammalian organs. Thus, changes in their quantities may influence the mechanochemical regulation of resident cells. Since maintenance of a native stromal composition is a requirement for three-dimensional (3D) matrix-based recellularization techniques in tissue engineering, we studied the influence of the decellularization detergents on these proteins in porcine kidney, liver, pancreas, and skin. Using a quick thawing/quick microwave-assisted decellularization protocol and two different detergents, sodium dodecyl sulfate (SDS) vs Triton X-100 (TX100), at identical concentration, variations in matrix conservation of stromal proteins were detected by liquid chromatography–mass spectrometry coupled to light and scanning electron microscopies, in dependence on each detergent. In all organs tested except pancreas, collagens were retained to a statistically significant level using the TX100-based protocol. In contrast fibrillin, elastin (except in kidney), and decorin (only in liver) were better preserved with the SDS-dependent protocol. Irrespective of the detergent used, laminin always remained at an irrelevant level. Our results prompt attention to the type of detergent in organ decellularization, suggesting that its choice may influence morphoregulatory inputs peculiar to the type of 3D bioartificial mammalian organ to be reconstructed.

Keywords: mass spectrometry, collagen, elastin, fibrillin, decorin, laminin

Impact Statement

Simple change of the protocol's main detergent leads to a very substantial difference in the panel of the stromal proteins detected by qualitative and semiquantitative mass spectrometry in acellular porcine matrices. This remarkable methodological variable promises to yield proteomic reference panels in a number of different species-specific acellular matrices allowing for selective retainment of peculiar mechanochemical inputs, to differently address the development of the seeded cells in relation to the type of organ to be bioartificially reconstructed.

[1]Food and Drug Department, University of Parma, Parma, Italy.
[2]Laboratory of Regenerative Morphology and Bioartificial Structures, Unit of Biomedicine, Biotechnology, and Translational Sciences, DIMEC, University of Parma, Parma, Italy.
[3]IMEM Istituto dei Materiali per l'Elettronica ed il Magnetismo, Consiglio Nazionale delle Ricerche, Parma, Italy.
[4]Division of Endocrinology, Diabetes, and Metabolism, Department of Medicine, Tufts Medical Center, Tufts University School of Medicine, Boston, Massachusetts, USA.

Introduction

In mammals fibrous and nonfibrous proteins, proteoglycans and glycosaminoglycans contribute to the formation of the interstitial and basement membrane (BM) extracellular matrix (ECM) or stromal matrix (SM) of their organs.[1] The SM plays a key role in regulating development, growth, and function of resident cells through mechanochemical interactions[2,3] whose those mediated by collagens, elastin, fibrillin, decorin, and laminin are of fundamental importance. Indeed, fibrillary collagens provide the primary three-dimensional (3D) ECM scaffold to each tissue/organ ensuring its 3D stability, resistance to deformation, and plasticity.[4]

Similarly, elastin contributes to ECM resilience and elasticity using as a template the glycoprotein fibrillin, the latter acting as a sheath to the developing central core of amorphous elastin fibers.[5,6] In contrast, the proteoglycan decorin resides in the interstitial ECM where it functions as a bridge between the microfibrillar interstitial proteins and membrane receptors/adhesion molecules such as integrins to stabilize cells in their 3D matrix environment, and prevent their neoplastic transformation.[7] Similarly, laminin is a trimeric protein of the BM that anchors the SM to the cells, and controls cell differentiation including that of stem cells leaving their niche during regeneration processes.[8]

Collectively, the ECM molecules give rise to a 3D microfibrillar network that provides an informational backbone for cells, an essential requirement for tissue engineering approaches based on decellularized stromal matrices eventually recellularized to give rise to functional bioartifical organs.[3,9,10] However, in the context of the decellularization methodologies, a very critical step resides in the chemical treatment used to remove cytoplasmic and nuclear material without adversely affecting composition, biological activity, and 3D macroscopic and microscopic architecture of the ECM.[2,3,11–14]

A number of chemical treatments have been proposed[1,15] among which the detergents sodium dodecyl sulfate (SDS) and Triton X-100 (TX100) have gained widespread acceptance despite their cytotoxicity. In fact efficient removal of chemicals from the SM becomes mandatory to favor adequate recellularization of the intact 3D stroma. Therefore, choice of washing steps like those based on microwave irradiation may account for reliable cleaning of the 3D SM within a limited procedural time.[16]

Finally accurate quantification of collagens, elastin, fibrillin, decorin, and laminin of the SM is very desirable to gain insights into how different amounts of specific ECM proteins act as a guide to induce *in vitro/ex situ* 3D self-assembly of seeded cells during recellularization.[17,18] To this aim, a number of different liquid chromatography/mass spectrometry (LC-MS/MS) techniques have been successfully used to quantify ECM proteins.[19–23]

Therefore, starting from the same thawing-based/microwave-assisted protocol, we have studied the effect of an SDS-dependent treatment with respect to a TX100-dependent treatment on the LC-MS/MS detection of collagens, elastin, fibrillin, decorin, and laminin in the decellularized SM of porcine kidney, liver, pancreas, and skin.

Methods

Reagents

SDS was from Lisapharma S.p.A (Como, Italy). TX100, sodium hydroxide (NaOH), ethylene diammino tetraacetic acid (EDTA), 2-propanol and Tris-HCl, trypsin (p.n. T1426), pepstatin A, proteinase K (p.n. P2308), iodoacetamide (IAA), dithiotreitol (DTT), HEPES, trifluoroacetic acid (TFA), bovine serum albumin (BSA), and dimethyl sulfoxide (DMSO) were all purchased from Sigma-Aldrich® (Darmstadt, Germany). Protein assay dye reagent concentrate was from Bio-Rad. LC-grade water, acetic acid, acetonitrile, analytical reagent grade formic acid (FA), urea, and ammonium bicarbonate (ABC) were purchased from Carlo Erba (Milan, Italy).

Porcine tissues

Fresh porcine tissues were taken from a slaughterhouse, cut into pieces of appropriate size, and stored at −20°C until use.

Microwave-assisted decellularization

Tissues were let to quickly thaw at room temperature (RT), sliced into 2 mm thick pieces, washed for 3 h in distilled water, and immersed in either Solution 1 (Sol 1) made with SDS (1%, w/v)—NaOH (0.05%, v/v) or Solution 2 (Sol 2) made with TX100 (1%, v/v) NaOH (0.05%, v/v). All solutions were kept at 37°C. Then, using a microwave oven (Sharp®), tissues were treated as given in Table 1.

Before immersion in the decellularization solutions (Sol 1 or Sol 2), skin was pretreated by incubation in a 70% solution of 2-propanol and microwaved with 20 pulses of 5 s each pulse. Finally, all samples were rinsed in distilled water for 4 h, and subjected to 560 W microwave pulses (10 pulses, 5 s each; dwell time: 1 min) until complete detergent removal.

Light microscopy

Decellularized matrices and quickly RT-thawed control tissues were fixed by immersion in 4% paraformaldehyde–phosphate buffered saline (PBS) for 24 h at 4°C, paraffin embedded, cut at the microtome (8 μm sections), stained with hematoxylin-eosin (HE), and analyzed using a Zeiss Axiophot light microscope under differential interference contrast (Nomarsky optic), and an AxioVision 4.8 image analysis software.

Scanning electron microscopy

Decellularized matrices were fixed in glutaraldehyde 2.5%–cacodylate sodium buffer 0.1 M overnight at 4°C, and rinsed

Table 1. Scheme of the Number of Microwave Pulses Performed for Each Tissue

	Sol 1—SDS	*Sol 2—TX100*
Tissue	*No. of pulses*[a]	
Kidney	100	190
Liver	200	200
Pancreas	150	130
Skin	180	220

Microwave power 560 W.
[a]Pulse duration: 5 s; dwell time: 1 min.

in PBS (0.1 M, pH 7.4). Two different though complementary scanning electron microscopy (SEM) modalities were used, in dependence on the type of decellularization (i.e., type of detergent used):

- with Sol 1, samples were dehydrated in graded series of ethanol, and subjected to critical point drying (Balzers) in a 100% ethanol/liquid CO_2 exchange system. Dried samples were mounted on aluminum stubs, metallized (Balzers apparatus) with a gold film, and observed with a Philips SEM 501.
- with Sol 2, samples were subjected to freeze drying for 24 h using a Christ Alpha 2-4 LSC plus freeze dryer. Dried samples were mounted on aluminum stubs, metallized (Balzers apparatus) with a gold film, and observed with a Zeiss Gemini SEM.

For each sample, both the surface and cross-section were studied. Representative images were analyzed using an ImageJ software (NIH, Bethesda, MD), and random measurements of putative blood vessel and corpuscular annexa were taken.

Analysis of the residual DNA content

Decellularized matrices and quickly RT-thawed control tissues were weighted and digested in 1 mL of lysis solution (LS) at 56°C for 48 h. The LS was composed of 1 mg/mL proteinase K in 50 mM Tris-HCl pH 7.6 and a protease inhibitor cocktail, made with 1 mM EDTA +1 mM IAA +10 μg/mL Pepstatin A diluted in DMSO. For DNA measurements, the CyQUANT® Cell Proliferation Assay kit (C7026; Invitrogen) was used. A calibration curve was prepared in a 96-multiwell plate using 200 μL serial dilutions (0, 62.5, 125, 250, 500, 1000 ng/mL) of the bacteriophage λ DNA in CyQUANT dye solution.

The latter was prepared by mixing the working buffer with the CyQUANT GR dye 400× supplied with the kit. For analysis, 5 μL of each digested sample (intact control and decellularized tissues) was dissolved in 195 μL of CyQUANT dye solution, and three replicates were prepared for each sample. Analyses of the calibration curve and samples were performed using a Victor 3V Multilabel Plate Readers (Perkin Elmer) set at the Fluorescein protocol (485/535 nm of wavelength—λ). The calibration curve was $y = 2296\ (\pm 94)\ x + 135{,}974\ (\pm 44{,}000)$ with an $R^2 = 0.993$. For each sample, the amount of DNA was normalized to the dilution factor and wet weight of the tissues and expressed as ng DNA/mg wet tissue.

Protein extraction and sample preparation for mass spectrometry analysis

One milligram wet weight of each decellularized sample was solubilized in a solution of 8 M urea–10 mM HEPES, immersed in an ultrasonic bath at 37°C for 3 h using a Bransonic ultrasonic cleaner 2510E-DTH, and sonicated at 42 kHz to break aggregates and extract proteins. Buffer exchange was performed using 50 mM ABC in Amicon Ultra 0.5 mL centrifugal filters (Sigma-Aldrich) with a 3-kDa molecular weight cut-off. Ensuing protein extracts, then, were assayed for protein dosage using the Bradford method, based on adding 10 μL of each sample to 500 μL of a previously diluted (1:5) Bradford reagent solution (absorbance = 595 nm). Calibration curve was achieved using a BSA standard (1 mg/mL) diluted to a range of 10–400 μg/mL ($y = 0.00108x$; $R^2 = 0.992$). Subsequently, proteins were reduced using 10 mM DTT (30 min at 37° C), alkylated by 25 mM IAA (30 min at RT in the dark), and the reaction was stopped by adding 10 mM DTT (15 min at RT). All samples were digested by incubation with trypsin (1:50 enzyme/substrate ratio) at 37°C overnight and, the digestion was stopped with 1 μL of FA added to each sample. Finally, samples were dried under nitrogen flow and reconstituted with 50 μL of a water–acetonitrile–FA aqueous solution (49.95/49.95/0.1, v/v). Each matrix sample was analyzed in triplicate.

LC-LIT-Orbitrap XL analysis

Tryptic separation of the digested proteins was carried out by using an XB C18 AERIS PEPTIDE (150 × 2.1 mm, 5 μm) column (Phenomenex, Torrance, CA) equipped with a prefiltering column. Eluting mixtures included solvents A (0.1% aqueous FA, v/v) and B (0.05% FA, 100% acetonitrile, v/v) delivered under gradient elution at the flow rate of 200 μL/min. Gradient was set as follows: 0 min 2% solvent B, 4 min 2% solvent B, 150 min 90% solvent B, 155 min 90% solvent B, and 170 min 2% solvent B.

The mobile phase was delivered by a Dionex Ultimate 3000 chromatographic system (Dionex Corporation, San José, CA) equipped with a 100-vial capacity sample tray. The volume of the injected samples was 5 μL. Qualitative protein analysis was obtained by mass spectrometry using an LTQ linear ion trap-Orbitrap XL instrument (ThermoScientific Corporation, San José, CA), equipped with ESI (ionization electrospray source) interface and controlled by Xcalibur software.

Optimized conditions of the interface were as follows: ESI voltage 3 kV, capillary voltage 13 V, capillary temperature 275° C, tube lens 100 V, sheath gas flow, auxiliary gas flow, and sweep gas flow delivered at 40, 10, and 5 arbitrary units, respectively. In the first scan event (full scan), the m/z window was 200–2000 with a resolution of 30,000. The four highest m/z ratios over threshold of 1000 counts were selected for collision-induced dissociation in the ion trap, with normalized collision energy of 35% in the collision cell.

LC-MS/MS SRM analysis

Relative quantitative analysis of SM proteins was carried out by LC-selected reaction monitoring (SRM)-MS/MS targeted analysis. Each SM tryptic solution was eluted by using a C18 Gemini (250 × 2.00 mm, 3 μm) column (Phenomenex) equipped with a C18 prefiltering column. An elution system based on a solvent gradient (solution A: 0.1% aqueous FA [v/v]/solution B: 0.08% FA in acetonitrile [v/v]) was delivered at 0.2 mL/min. The gradient elution program was as that described in the previous section. The mobile phase was delivered by the Agilent HP 1200 chromatographic system (Agilent Technologies) equipped with a 100-vial capacity sample tray.

Injection volume was 10 μL. A QTRAP 4000 triple quadrupole mass spectrometer (ABSCIEX, Foster City, CA), equipped with a pneumatically assisted ESI interface, was used. The sheath gas (nitrogen, 99.999% purity) and the auxiliary gas (nitrogen, 99.998% purity) were delivered at flow rates of 45 and 5 arbitrary units, respectively. Optimized conditions of the

interface were as follows: ESI voltage 5.5 kV, capillary voltage 50 V, and capillary temperature 350°C. Experiments were performed under positive ion-SRM conditions using nitrogen as collision gas (pressure of 2.1×10^{-3} mbar) and a 20 ms-dual time for each transition monitored.

Data analysis, bioinformatics, and quantitative evaluation of ECM peptides

LC-LIT-Orbitrap XL data were processed using PEAKS X+ software (Bioinformatics Solutions, Inc., Waterloo, Canada) and Uniprot as protein database (www.uniprot.org, protein sequence database; *sus scrofa*) setting trypsin as digestion mode with three as maximum number of post-translational modifications per peptide, no limit to possible modifications and false discovery rate active. For SRM-targeted analysis, *in silico* evaluation of protein sequences was performed as follows: FASTA protein sequences were obtained from Uniprot Porcine proteome database, and SRM transitions for each protein were simulated by Skyline (v. 20.1; SCIEX, Redwood City, CA), setting trypsin as digestion mode with no missed cleavage and carbamidomethylation of cysteines as structural modification.

Uniqueness of candidate peptide sequences was assessed by BLASTp tool (basic local alignment search tool; www .ncbi.nml.nih.gov NCBI BLAST) search (algorithm: blastp; ATRIX PA 30; GAP COASTS: existence 10, extension 1; DATABASE: nonredundant protein sequences) from NCBI (National Center for Biotechnology Information, Bethesda, MA). LC-MS/MS SRM data were analyzed using the Analyst v 1.4 software, and integrations of the peak areas were obtained by the MultiQuant program (version 2.1; ABSCIEX).

All samples were processed with the same extraction protocol resulting in the final clean tryptic digests ready for LC-MS/MS analysis. Relative quantitation of SM peptides was achieved through normalization of data with respect to total protein content measured for each sample by Bradford analysis before enzymatic digestion and expressed as the value of the area (intensity of ionic current or cps/min) under each MS peak. This unit of measurement was reported as ''scientific notation'' or E series.

Statistical analysis

Differences in ng DNA/mg wet weight between controls and decellularization protocols were calculated after an initial estimate of the sample dry weight, based on the assumption of a 60% decrease in the experimentally recorded weight, as currently accepted. Then using a 2×2 chi squared test, ng DNA/mg dry weight above or below a threshold recommended as ideal for decellularization[15] was compared. In contrast, differences in the quantity of cumulated SM collagens and proteins, and selective SM elastin, fibrillin, decorin, and laminin sequences between decellularization protocols were determined using one-way analysis of variance. All results were considered significant if $p < 0.05$.

Experiment

Both control and treated tissue samples were subjected to the methods previously detailed.

Figure 1 shows that irrespective of the decellularization protocol, all treated samples resulted devoid of visible cellular material as opposed to control tissues retaining the native parenchymal and vascular structure. In intact kidney, renal glomerula were surrounded by convoluted tubules as compared with the absence of any recognizable cellular structure in decellularized matrices, consisting of a fibrous stromal network. Similarly, in intact live, blood vessels were surrounded by parenchymal trusses as compared with the absence of any recognizable cellular structure in the decellularized matrices, depicting the stromal scaffold of cellular cords and vessels.

In control pancreas, cords of exocrine pancreatic cells were well preserved as compared with decellularized matrices, retaining the tissue stromal structure including that of blood vessels. Finally, as in the control skin, the dermal structures were readly recognized in decellularized tissues, that exhibited a dermal fibrous structure and walls of blood vessels.

Figure 2 shows the ultrastructural appearance of decellularized tissue matrices. Irrespective of the decellularization protocol applied and SEM technology used, all decellularized tissues depicted a well-preserved 3D stromal architecture devoid of any visible cellular residue, while retaining stromal septa and spaces of presumptive vascular conduits and corpuscular annexa. Indeed, in all types of matrix, random linear measurements revealed open lumina (30–200 μm in diameter), anatomically compatible with either small blood vessels and their curling up (kidney, liver, pancreas) or cavities of annexa like hair follicles (skin).

Figure 3 shows that the majority of decellularized tissues reached a statistically significant reduction in residual DNA with respect to the already low level of DNA in control tissues, the latter as an expected result of the quick defrost of the frozen samples. Indeed, the thawing procedure was *per se* able to favor abundant detachment of cells by the SM, up to reduce tissue DNA below the ideal threshold of 50 ng DNA/mg dry weight (corresponding to 41.5 ng DNA/mg wet weight) in control kidney and pancreas. However, using the SDS-based protocol (Sol 1), a statistically significant reduction of matrix DNA was achieved in kidney, liver, and skin with respect to controls. In contrast, using the TX100-based protocol (Sol 2), a statistically significant reduction of matrix DNA was achieved in pancreas and skin.

Supplementary Table S1 shows that using LC-LIT-Orbitrap XL analysis, collagens types I–VI, XII, XIV and laminin subunits alpha 5, beta 1, and beta 2 were readily identified. Among different SM, a peculiar distribution of these molecules was observed, variable in dependence on the organ analyzed and within the same type of organ related to the detergent used for decellularization. However, irrespective of the decellularization detergent, sharing of identical molecules between organs accounted for only 3.7% of the total detected proteins, highlighting conservation of the structural uniqueness of each SM with respect to its native tissue.

Supplementary Table S2 highlights in bold the peptide sequences tested using LC-MS/MS SRM analysis. Among the numerous available, only those having the best characterized chromatographic peaks were selected for quantification and comparison between decellularization procedures.

Figure 4 shows that in all matrices except pancreas, a higher statistically significant collagen retention was observed

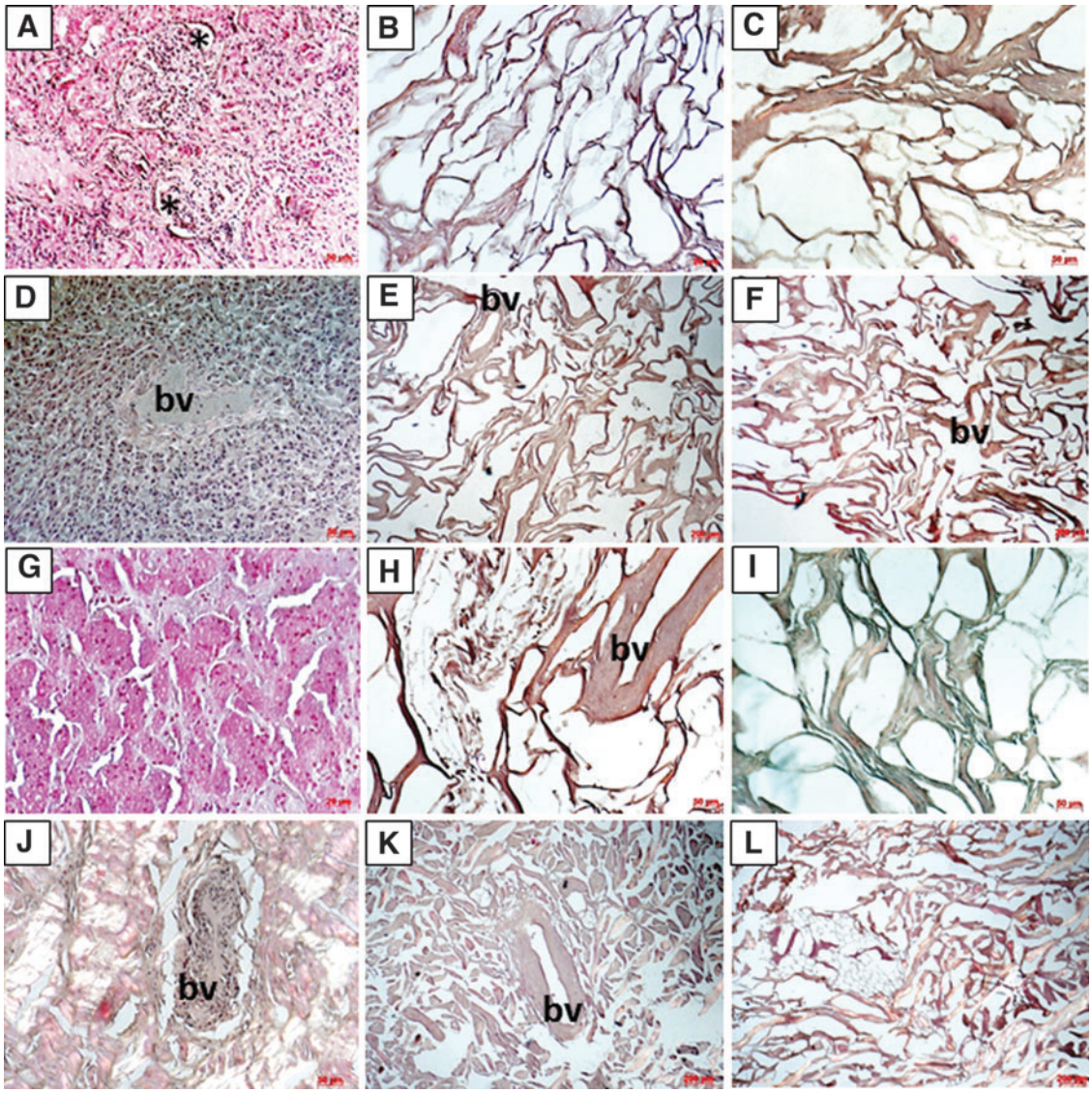

FIG. 1. Light microscopic evidence for removal of cellular debris in decellularized matrices: **(A)** control kidney (*asterisk* shows a glomerulus), **(B, C)** decellularized kidney treated with Sol 1 **(B)** and Sol 2 **(C)**. **(D)** Control liver, **(E, F)** decellularized liver treated with Sol 1 **(E)** and Sol 2 **(F)**; **(G)** control pancreas, **(H, I)** decellularized pancreas treated with Sol 1 **(H)** and Sol 2 **(I)**; **(J)** control skin, **(K, L)** decellularized skin treated with Sol 1 **(K)** and Sol 2 **(L)**. *Red* size markers: **(A, C, D, H, I, J)** = 150 μm; **(B, G)** = 50 μm; **(E, F, K, L)** = 400 μm. Each image refers to a prototypical tissue sample. bv, blood vessels; Sol 1, Solution 1; Sol 2, Solution 2.

with Sol 2 as opposed to Sol 1. In contrast, Figure 5 shows the semiquantitative cumulated results of all subunit/isoforms of the stromal (SM) proteins, in all matrices. In particular, a statistically significant higher amount of these SM proteins was retained using Sol 1 as opposed to Sol 2.

Finally, Figure 6 shows that in all organ matrices, a statistically significant higher amount of fibrillin was retained using Sol 1; similarly in liver, pancreas, and skin, also elastin (isoforms X1–X26) was equally preserved at a higher statistically significant level using Sol 1. However, only in liver, decorin remained at a higher statistically significant level using Sol 1. At variance, laminin (subunit alpha 5 isoforms X1 and X2) was never retained to either a statistically significant level or even to a simply detectable level in any of the tested matrices and irrespective of the protocol used.

Discussion

Collagens and proteins/proteoglycans such as elastin, fibrillin, decorin, and laminin represent key ECM molecules for 3D organ reconstruction in tissue engineering based on recellularization of decellularized organ's matrices with stem cells/progenitors.[24] Depending on the molecular composition of the decellularized SM, different patterns of cell self-assembly can be expected during *ex situ* organ reconstruction.[25,26] In addition, the availability and quantity of SM collagens depend on the decellularization procedure and primarily by the chemical detergents used for cell detachment/removal, as we have recently shown in decellularized rat thyroid matrices.[14]

Therefore, based on a common and standard physical approach for quick breaking of cell–matrix fibrous bonds

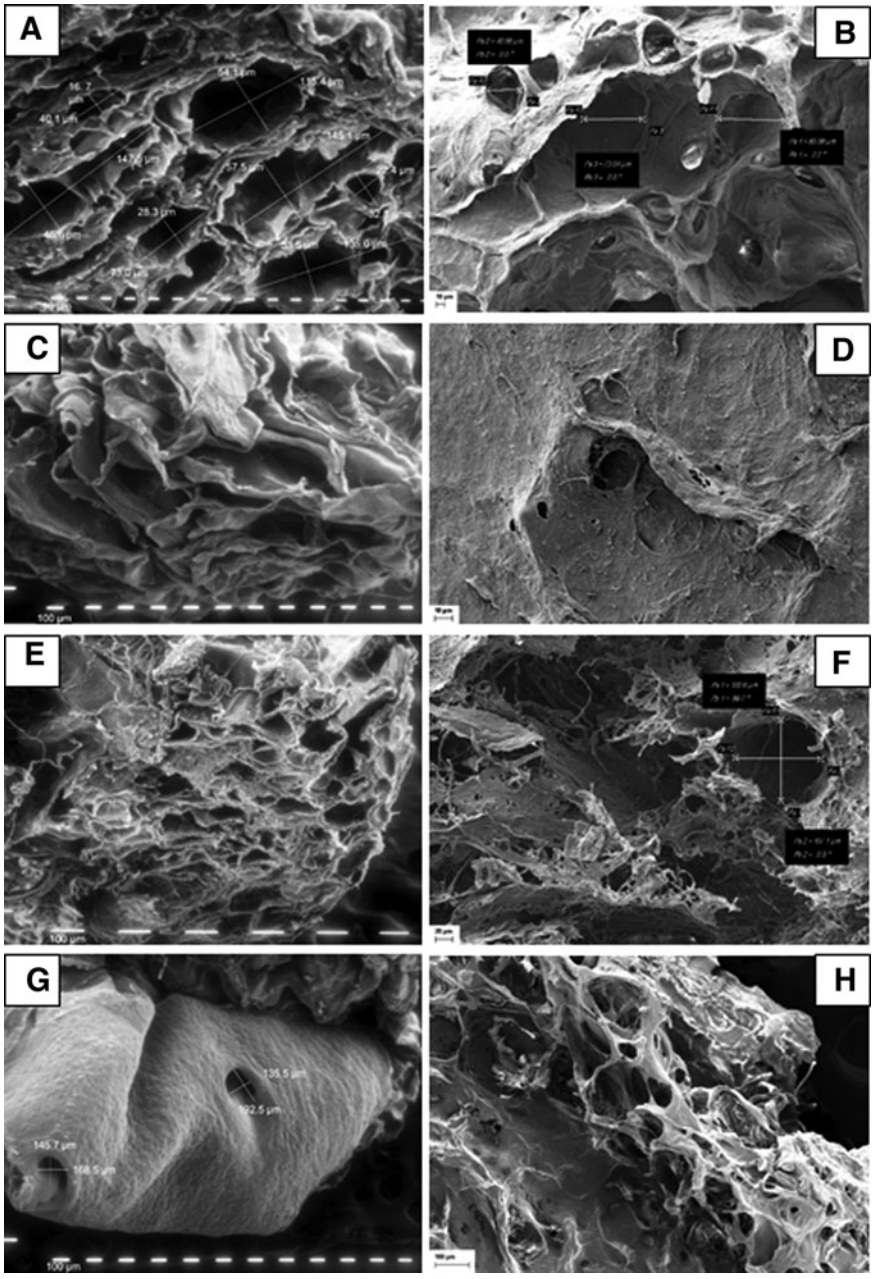

FIG. 2. SEM evidence for removal of cellular debris in decellularized matrices: **(A)** kidney cross section treated with Solution 1—Sol 1; **(B)** kidney cross section treated with Sol 2; **(C)** liver cross section treated with Sol 1; **(D)** liver surface treated with Sol 2; **(E)** pancreas cross section treated with Sol 1; **(F)** pancreas cross section treated with Sol 2: **(G)** skin surface treated with Sol 1; **(H)** skin cross section treated with Sol 2. Size markers: **(A, C, E, G)** = 100 μm; **(B)** = 25 μm; **(D)** = 15 μm; **(F)** = 25 μm; **(H)** = 100 μm. Each image refers to a prototypical tissue sample. SEM, scanning electron microscopy.

and cleaning of the SM from cellular debris, we have focused on the role played by two different and widely used chemical detergents (SDS and Triton-X) in influencing availability and quantities of SM proteins in decellularized 3D matrices of pig. This, with the intent to provide SM models suitable for 3D reconstruction of human organs for transplantation replacement[10] and to initiate a standardization of the decellularization method for eventual human applications.

To this aim, we decided to use identical concentrations and times of application of the detergent solutions. In this manner, it has been possible to readily verify the effects of the detergents on a number of structural parameters of the decellularized matrices, potentially relevant for their recellularization.

Remarkably, both SDS- and TX100-based preparations led to a light microscopic and ultrastructural evidence of comparable and adequate preservation of the 3D SM fibrous structures, and apparent removal of all cell nuclear material. However, more detailed analysis of the residual DNA content revealed that only the skin matrix reached a satisfactory DNA removal, that is, below the internationally accepted threshold of 50 ng DNA/dry weight[15] with either SDS or TX100. Specifically, the ionic detergent SDS is ideal for protein denaturation as opposed to the nonionic detergent TX100 whose properties favor rupture of lipid–protein and lipid–lipid interactions.[27]

Since pancreas has the highest lipid content with respect to liver and kidney in both pig and man,[28,29] it is presumed that the highest efficiency of TX100 on the pancreatic matrix ensued from its more striking lipolytic action as opposed to SDS, which proved to be more effective in tissues such as kidney and liver harboring an abundant protein concentration.[30]

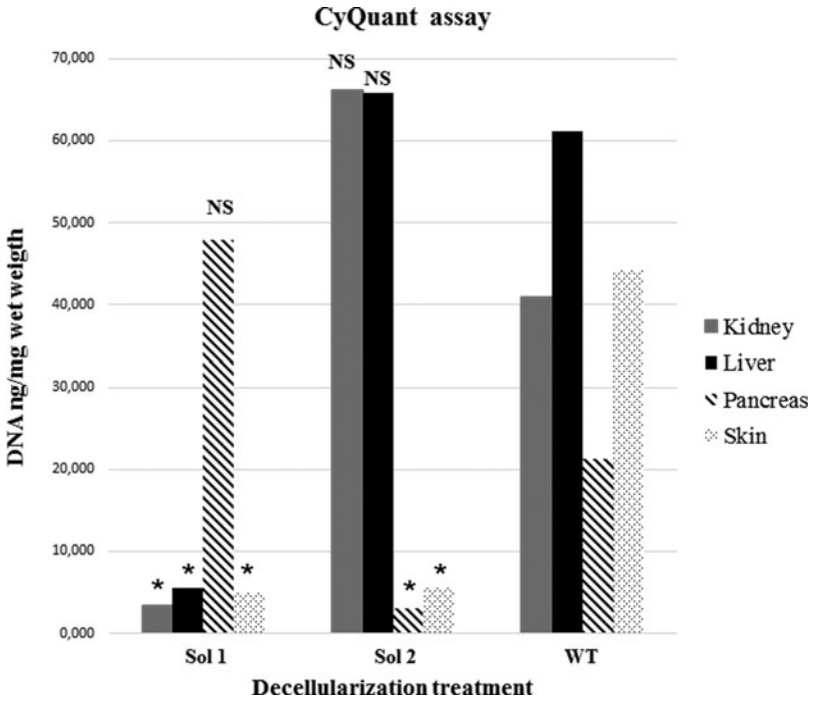

FIG. 3. Distribution of residual nuclear material (DNA) in decellularized matrices as compared with quickly RT-thawed control tissues. Each bar represents a single representative tissue sample, thus no error bar is depicted. *$p < 0.05$; NS, not statistically significant; RT, room temperature.

In addition, since nuclear lipids give rise to a ''morpho-functional shelter'' to nucleic acids instrumental to DNA translation and gene transcription,[31] inadequate removal of lipids from the nuclear compartment may have contributed to an insufficient denaturation of the DNA helix, which remained entrapped inside its natural lipid scaffold.[32] At a tissue level, these assumptions are confirmed by the ability of both detergent solutions to yield a satisfactory DNA removal from the skin matrix whose very rich lipid layer was detached by pretreatment with a lipid solvent (2-propanol 70%).

The key role played by the detergents in the preparation of each organ's matrix was further confirmed by mass spectrometry analysis. In particular using TX100, collagen types I–VI were better retained in liver, kidney, and skin, whereas no differences were observed in pancreas as compared with SDS. Collagen types I, II, III, and V play a key role in ensuring tensile strength and 3D stability of the SM including their 3D assembly with fibril-associated collagen types XII and XIV.[4] Differently, collagen type IV is a network-forming collagen residing in the BM where it forms a reticular network to promote cell attachment and connection to other local proteins.[33–35]

Finally, collagen type VI is particularly abundant in parenchymal organs such as the kidney glomerulus, and involved in both mechanical and cell growth-regulating activities.[17] Therefore, we suggest that availability of these collagens may play a critical role during 3D *ex situ* recellularization of matrices requiring a specific 3D geometry for organ's strength. This is the case of *in vivo* liver, kidney, and skin dealing with anatomical constraints and/or dynamic insults as opposed to pancreas, which is physically protected in the abdomen by the surrounding viscera.

As a consequence, a TX100-based decellularization protocol would ideally fit with the preparation of liver, kidney, and skin 3D matrices. In the liver, then, this approach

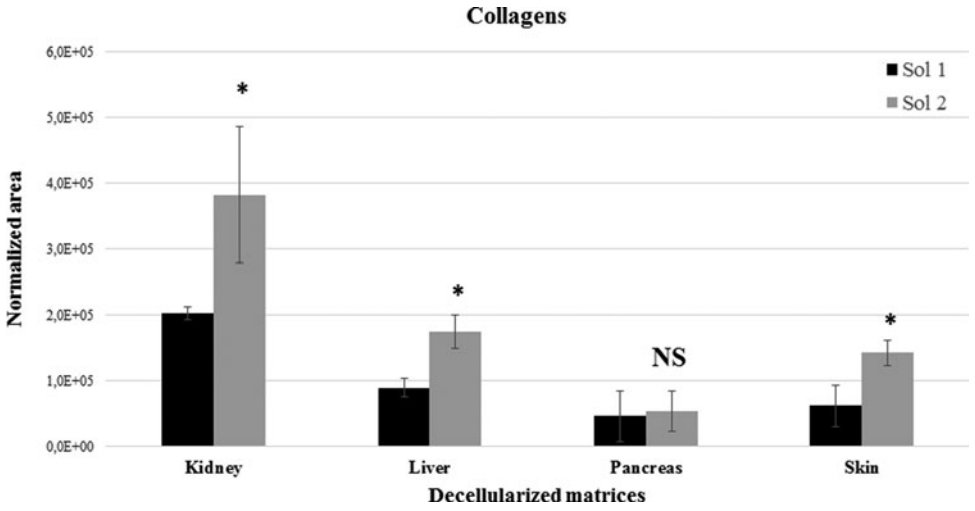

FIG. 4. Cumulated distribution of collagens types I–VI (including their isoforms) in each decellularized tissue using Sol 1 (SDS-based protocol) versus Sol 2 (TX100-based protocol), as determined by LC-MS/MS SRM analysis. *$p < 0.05$; data are the mean ± SD of three independent samples. LC-MS/MS, liquid chromatography/mass spectrometry; SD, standard deviation; SDS, sodium dodecyl sulfate; TX100, Triton X-100.

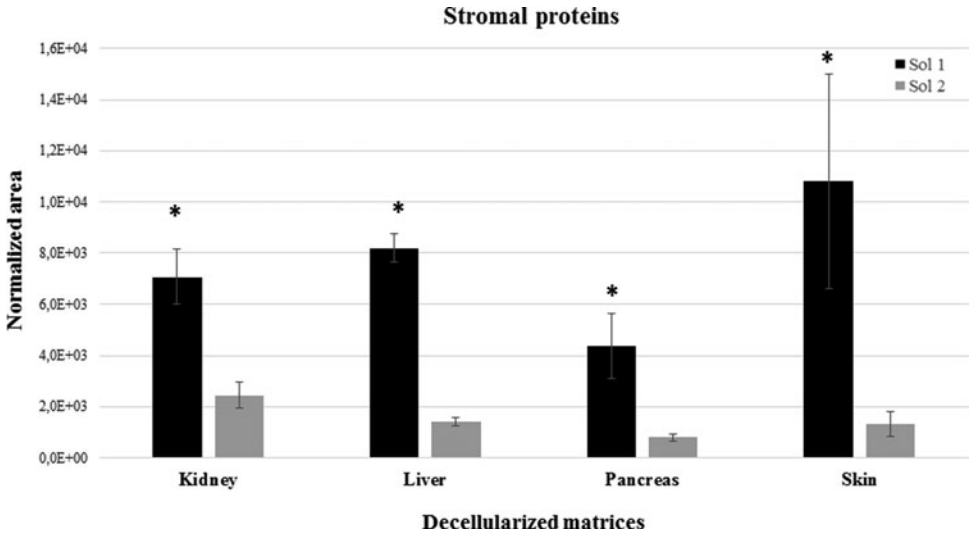

FIG. 5. Cumulated distribution of stromal proteins (including their subunits/isoforms) elastin, fibrillin, decorin, and laminin in each decellularized tissue using Sol 1 (SDS-based protocol) versus Sol 2 (TX100-based protocol), as determined by LC-MS/MS SRM analysis. $*p < 0.05$; data are the mean ± SD of three independent samples.

additionally favored high conservation of the interstitial proteoglycan decorin, able to regulate endothelial cell autophagy and cell proliferation,[7] two functional properties shared with collagen type IV[33] to ensure structural stability of the wide hepatic vascular field, as confirmed in recent studies on mammalian liver and kidney.[36–38]

Differently, using SDS, a better conservation occurred to all the identified elastin isoforms (except for kidney) and fibrillin in all matrices tested. Elastin and its associated protein fibrillin regulate elastic module and deformability of the SM through mechanochemical interactions with a number of extracellular glycoproteins to ensure adequate tissue remodeling during organ's regeneration.[5,6] Therefore, our results suggest that an SDS-based protocol would ideally fit for the 3D *ex situ* recellularization of matrices requiring an high deformability for *in vivo* organ's activity such as skin, but also viscera, enriched with arteries including liver, kidney, and pancreas might equally benefit of it.

Finally, none of the two protocols tested was able to retain the glycoprotein laminin (subunit alpha 5 isoforms X1 and X2) in any of the matrices studied. Laminin anchors the BM to the SM, and promotes homing and survival of stem cells in their local tissue niche,[8] indeed, it has been found to *in vitro* stimulate morphogenesis of pancreatic endocrine islets from mouse pancreatic ductal cells *in vitro*,[39] suggesting that its loss in decellularized matrices might hamper growth and differentiation of precursor cells during recellularization. Thus, different and/or less aggressive decellularization approaches should ideally be developed to sufficiently preserve laminin in all these matrix types, particularly if recellularization is planned to occur using stem cells/progenitors.

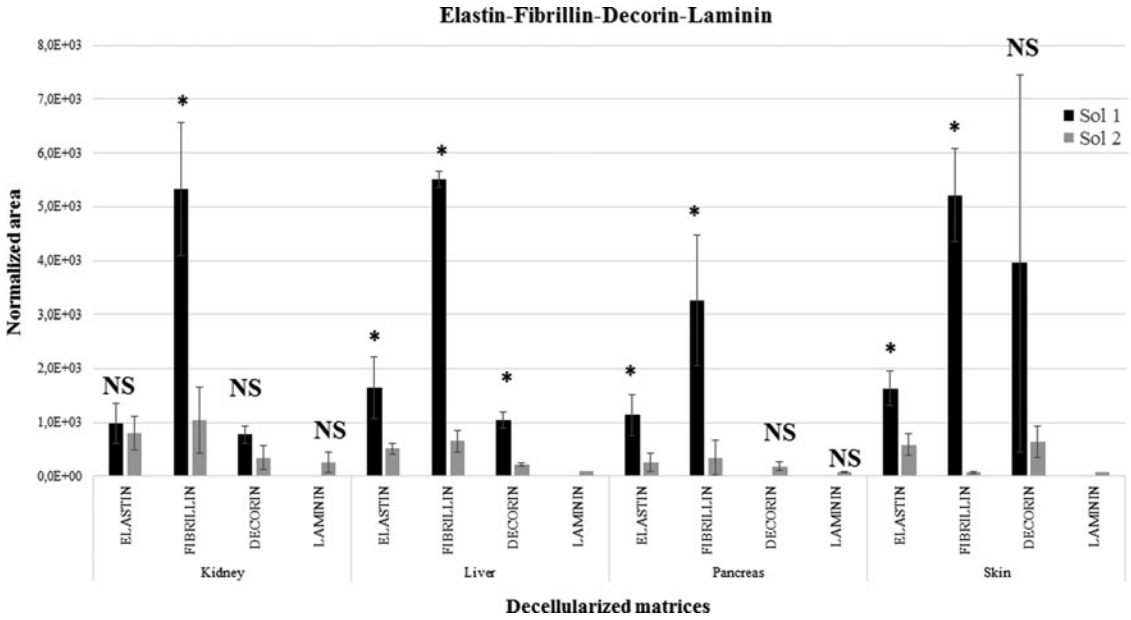

FIG. 6. Selective distribution of the stromal proteins elastin (isoforms X1–X26), fibrillin, decorin, and laminin (subunit alpha 5 isoforms X1 and X2) in each decellularized tissue using Sol 1 (SDS-based protocol) versus Sol 2 (TX100-based protocol), as determined by LC-MS/MS SRM analysis. $*p < 0.05$; data are the mean ± SD of three independent samples, except for laminin in liver and skin where it was found only in one single sample.

In conclusion, our study has enlightened the very selective action of two widely used chemical detergents in tissue decellularization, SDS and TX100. Starting from a common tissue-breaking and similar washing steps through microwave irradiation, we showed that relevant quantitative differences occurred to key fibrous and nonfibrous extracellular and/or basal membrane proteins of porcine liver, kidney, pancreas, and skin in dependence on the detergent used.

Since pig matrices may find application in transplantation therapy as natural scaffolds for engineering of human organs, and each detergent allows for saving selective morphoregulatory and mechanochemical ECM patterns, hints have been provided for optimized preparation of these 3D matrices eventually to be used as tools for recellularization of 3D bioartificial human organs.

Authors' Contributions

G.R. contributed to mass spectrometry and analytical studies and article writing. F.B. and G.C. were involved in DNA analysis and light and ultrastructural SEM investigations. G.T. carried out SEM studies. C.B. was in charge of mass spectrometry/analytical investigations. R.T. was involved in article supervision including English language. L.E. carried out research conceptualization, project administration, methodology, data evaluation, and article revision.

Acknowledgment

This study is dedicated to the memory of Davide Dallatana who enthusiastically contributed to this and many other scientific investigations of our groups during the past 15 years providing essential technical and scientific expertise. The authors thank Dr. Martina Calestani for the excellent technical assistance.

Disclosure Statement

No competing financial interests exist. G.R. is recipient of a 2019–2022 research fellowship in the PhD course of drug science, under the tenure of the EU Grant Horizon 2020 SCREEENED #825745.

Funding Information

The author(s) disclosed receipt of the following financial support for the research, authorship, and/or publication of this article: Part of this research was conducted under the support of the UNIPR-FIL 2018–2020 fund.

Supplementary Material

Supplementary Table S1
Supplementary Table S2

References

1. Frantz, C., Stewart, K.M., and Weaver, V.M. The extracellular matrix at a glance. J Cell Sci **123,** 4195, 2010.
2. Kim, S.H., Turnbull, J., and Guimond, S. Extracellular matrix and cell signalling: the dynamic cooperation of integrin, proteoglycan and growth factor receptor. J Endocrinol **209,** 139, 2011.
3. Edelman, G.M. Morphoregulation. Dev Dyn **193,** 2, 1992.
4. Ricard-Blum, S. The collagen family. Cold Spring Harb Perspect Biol **3,** 1, 2011.
5. Thomson, J., Singh, M., Eckersley, A., *et al.* Fibrillin microfibrils and elastic fibre proteins: functional interactions and extracellular regulation of growth factors. Semin Cell Dev Biol **89,** 109, 2019.
6. Kristensen, J.H., and Karsdal, M.A. Elastin. In: Biochemistry of Collagens, Laminins and Elastin. Germany: Elsevier, Inc., 2016, 30, pp. 197–201. DOI: 10.1016/B978-0-12-809847-9.00030-1.
7. Gubbiotti, M.A., Vallet, S.D., Ricard-Blum, S., *et al.* Decorin interacting network: a comprehensive analysis of decorin-binding partners and their versatile functions. Matrix Biol **55,** 7, 2016.
8. Yap, L., Tay, H.G., Nguyen, M.T.X., *et al.* Laminins in cellular differentiation. Trends Cell Biol **29,** 987, 2019.
9. Sadrabadi, A.E., Baei, P., Hosseini, S., *et al.* Decellularized extracellular matrix as a potent natural biomaterial for regenerative medicine. Adv Exp Med Biol **1341,** 27, 2021.
10. Atala, A. Engineering organs. Curr Opin Biotechnol **20,** 575, 2009.
11. Hrebikova, H., Diaz, D., and Mokry, J. Chemical decellularization: a promising approach for preparation of extracellular matrix. Biomed Pap **159,** 12, 2015.
12. Toni, R., Bassi, E., Barbaro, F., *et al.* Bioartificial endocrine glands: at the cutting edge of translational research in endocrinology. In: Sprio, S., and Tampieri, A., eds. Bio-Inspired Regenerative Medicine: Material, Processes, and Clinical Applications. Singapore: Pan Standford Publishing, 2016, p. 357.
13. Toni, R., Tampieri, A., Zini, N., *et al.* Ex situ bioengineering of bioartificial endocrine glands: a new frontier in regenerative medicine of soft tissue organs. Ann Anat **193,** 381, 2011.
14. Alfieri, M., Barbaro, F., Consolini, E., *et al.* A targeted mass spectrometry method to screen collagen types I-V in the decellularized 3D extracellular matrix of the adult male rat thyroid. Talanta **193,** 1, 2019.
15. Gilbert, T.W., Sellaro, T.L., and Badylak, S.F. Decellularization of tissues and organs. Biomaterials **27,** 3675, 2006.
16. Fujisato, T., Kishida, A., Funamoto, S., *et al.* Method of treating biological tissue by microwave-irradiation, United States Patent. Patent No.: US 7,883,864 B2. Date of Patent: 8 February, 2011. USOO7883864B2.
17. Cescon, M., Gattazzo, F., Chen, P., *et al.* Collagen VI at a glance. J Cell Sci **128,** 3525, 2015.
18. Jakab, K., Neagu, A., Mironov, V., *et al.* Engineering biological structures of prescribed shaped using self-assembling multicellular systems. Proc Natl Acad Sci U S A **101,** 2864, 2004.
19. Pataridis, S., Eckhardt, A., Mikulíková, K., *et al.* Identification of collagen types in tissues using HPLC-MS/MS. J Sep Sci **31,** 3483, 2008.
20. Johnson, T.D., Hill, R.C., Dzieciatkowska, M., *et al.* Quantification of decellularized human myocardial matrix: a comparison of six patients. Proteomics Clin Appl **10,** 75, 2016.
21. Goddard, E.T., Hill, R.C., Barrett, A., *et al.* Quantitative extracellular matrix proteomics to study mammary and liver tissue microenvironments. Int J Biochem Cell Biol **81,** 223, 2016.
22. Liu, X., Guo, Z., Sun, H., *et al.* Comprehensive map and functional annotation of human pituitary and thyroid proteome. J Proteome Res **16,** 2680, 2017.

23. Chahrour, O., Cobice, D., and Malone, J. Stable isotope labelling methods in mass spectrometry-based quantitative proteomics. J Pharm Biomed Anal **113,** 2, 2015.
24. Park, K.M., and Woo, H.M. Systemic decellularization for multi-organ scaffolds in rats. Transplant Proc **44,** 1151, 2012.
25. Toni, R., Della Casa, C., Spaletta, G., *et al.* The bioartificial thyroid: a biotechnological perspective in endocrine organ engineering for transplantation replacement. Acta Biomed **78,** 129, 2007.
26. Sprio, S., Sandri, M., Iafisco, M., *et al.* Biomimetic materials in regenerative medicine. In: Biomimetic Biomaterials: Structure and Applications. Germany: Elsevier Limited, 2013, pp. 3–45.
27. Johnson, M. Detergents: Triton X100, Tween-20, and more. Mat Meth **163,** 3, 2013.
28. Seong, P.N., Kang, G.H., Park, K.M., *et al.* Characterization of edible pork by-products by means of yield and nutritional composition. Korean J Food Sci An **34,** 297, 2014.
29. Sijens, P.E., Edens, M.A., Bakker, S.J.L., *et al.* MRI-determined fat content of human liver, pancreas and kidney. World J Gastroenterol **16,** 1993, 2010.
30. Crapo, P.M., Gilbert, T.W., and Badylak, S.F. An overview of tissue and whole organ decellularization processes. Biomaterials, **32,** 3233, 2011.
31. Maraldi, N.M., Zini, N., and Squarzoni, S. Morphological evidence of function-related localization of phospholipids in the cell nucleus. Adv Enzyme Regul **32,** 73, 1992.
32. Maraldi, N.M., Zini, N., Santi, S., *et al.* Topology of inositol lipid signal transduction in the nucleus. J Cell Physiol **181,** 203, 1999.
33. Kühn, K. Basement membrane (type IV) collagen. Matrix Biol **14,** 439, 1995.
34. Söder, S., and Pöschl, E. The NC1 domain of human collagen IV is necessary to initiate triple helix formation. Biochem Biophys Res Commun **325,** 276, 2004.
35. Toni, R. Topobiology: epistemological implications of an ontic theory in biomorphology. It J Philos Sci Epistemologia **27,** 83, 2004.
36. Baptista, P.M., Orlando, G., Mirmalek-Sani, S.H., *et al.* Whole organ decellularization—a tool for bioscaffold fabrication and organ bioengineering. Annu Int Conf IEEE Eng Med Biol Soc **2009,** 6526, 2009.
37. Kajbafzadeh, A.M., Javan-Farazmand, N., Monajemzadeh, M., *et al.* Determining the optimal decellularization and sterilization protocol for preparing a tissue scaffold of a human-sized liver tissue. Tissue Eng Part C Methods **19,** 642, 2013.
38. Sharma, R., Greenhough, S., Medine, C.N., *et al.* Three-dimensional culture of human embryonic stem cell derived hepatic endodermand its role in bioartificial liver construction. J Biomed Biotechnol **2010,** 236147, 2010.
39. Boretti, M.I., and Gooch, K.J. Effect of extracellular matrix and 3D morphogenesis on islet hormone gene expression by Ngn3-infected mouse pancreatic ductal epithelial cells. Tissue Eng Part A **14,** 1927, 2008.

Address correspondence to:
Lisa Elviri, PhD
Food and Drug Department
University of Parma
Parco Area delle Scienze 27/a
43124 Parma
Italy

E-mail: lisa.elviri@unipr.it

Received: January 14, 2022
Accepted: March 18, 2022
Online Publication Date: April 18, 2022